

# Using Ultrasonography to Define Fetal–Maternal Relationships: Moving from Humans to Mice

Jianhong Zhang and B Anne Croy\*

Ultrasound scanning is a noninvasive, accurate, and cost-effective method to create images of the female reproductive tract clinically and in research. Ultrasonography is particularly valuable for studying the dynamic relationships among mother, placenta, and fetus during pregnancy because this modality does not disturb the ongoing course of gestation. Importantly, the complex vascular changes in the mother induced by pregnancy and the vascular system generated to support placental function can be assessed quantitatively and functionally by ultrasonography. Many mouse models are available that address aspects of human placental function and dysfunction, but high-quality microultrasound technology suitable for use in pregnant mice has become widely available only recently. This technical advance now enables real-time recording of maternal–fetal interactions in pregnant rodents. The ability to perform microultrasonic analyses of parameters such as uterine arterial remodeling, hemodynamic changes, placental development, and fetal growth in mice now permits research that uses the same imaging platform as that for human patients. This capability will enhance the translation of information derived from rodent studies to the clinic.

**Abbreviations:** gd, gestation day; IUGR, intrauterine growth restriction.

Human pregnancy is a complex, dynamic process accompanied by both inspiring and amazing events. Clinically, disorders of pregnancy are among the least understood areas in health science because of ethical and cultural challenges and the involvement of 2 (or more) subjects (mother and fetus) rather than 1. Because continuation and successful conclusion of pregnancy typically are desired, advances in clinical and research investigations of human pregnancy are highly dependent upon technological advances in noninvasive imaging. The most common human gestational complications are preeclampsia (acute onset of hypertension during the second half of pregnancy), intrauterine growth restriction (IUGR), and diabetes. These pathologies are thought to share many risk factors, particularly an inadequate response of the maternal vasculature to the state of pregnancy.<sup>59</sup> In all mammals, maternal vascular adaptation is essential to meet the requirements of blastocyst implantation and placental and fetal development to ensure a successful pregnancy. In species with hemochorial placentation (including human, rat, and mouse), endometrial decidualization is associated with maternal vascular remodeling at implantation sites, and the remodeling process has become a diagnostic and therapeutic target.<sup>39,47</sup>

Ultrasonography was introduced in 1958 and has become the diagnostic tool of choice to study human gestational health,<sup>18</sup> not only because this modality is noninvasive with very low risk but also because it provides real-time images with positional information.<sup>24</sup> Ultrasonography is relatively inexpensive and portable, compared with other modalities such as MRI and computed tomography. Modern clinical ultrasonography usually is performed by using a pulse–echo approach with a brightness-mode (B-mode)

output that can be augmented by using advanced functions such as color Doppler mapping, 3D or 4D imaging, and spectral measurements. Application of these ultrasound techniques has enabled exploration and understanding of human maternal–fetal relationships that previously had been virtually inaccessible. Most studies of the physiology and pathology of pregnancy in animal models still rely on postmortem approaches rather than serial examinations, which would decrease experimental animal numbers. A key advance for studies of pregnancy in mice has been the development of microultrasonography. This technology now provides *in vivo* morphometric quantification of embryonic and placental growth for mice.<sup>21,33</sup> Here we review the application of microultrasonography to hemodynamic monitoring, vascular assessment, and placental development in mice and address its limitations briefly.

**Cardiovascular modifications of normal pregnancy.** Transient, systemic, physiologic changes to the cardiovascular system are an immediate consequence of mammalian pregnancy. These include cardiac acceleration, blood volume expansion, and angiogenesis. However, the greatest differences vasodilation and angiogenesis occur in vessels of the reproductive tract.<sup>71</sup> Increased uterine vascular permeability is a hallmark of implantation in mice, a process that initiates endometrial decidualization and angiogenesis. Vascular endothelial growth factor,<sup>52,54</sup> placenta growth factor,<sup>16</sup> matrix metalloproteinase,<sup>36</sup> shear force,<sup>19</sup> ovarian hormones,<sup>57</sup> and endothelial NO synthase<sup>55</sup> are among the factors involved in these processes. Hypertrophic remodeling of uterine arteries occurs and includes transient phenotypic modulation and proliferation of smooth muscle cells and alterations in the composition of the extracellular matrix.<sup>56</sup>

In most mammals, blood is delivered to the uterus bidirectionally by means of a dual arterial anastomosing loop arising from the ovarian and internal iliac arteries. Unlike the linear, branch-

Received: 11 Aug 2009. Revision requested: 11 Sep 2009. Accepted: 28 Sep 2009.  
Department of Anatomy and Cell Biology, Queen's University, Kingston, Ontario, Canada.

\*Corresponding author. Email: Croya@queensu.ca

ing pattern of most vascular networks, where blockage leads to downstream ischemia, the bilateral arrangement provides the mammalian uterus with redundancy in case of vascular occlusion.<sup>39</sup> The uterine arteries travel into the inner myometrium as the spiral arteries.<sup>43</sup> During early pregnancy in humans, the spiral arteries undergo vast structural changes, through loss of the normal musculoelastic components of the arterial wall and their replacement by amorphous fibrinoid material. Extravillous trophoblast cells and decidual leukocytes participate in these normal physiologic changes,<sup>50</sup> which are linked to pregnancy success. Incompleteness in these processes is associated strongly with the acute-onset, hypertensive emergency of human pregnancy called 'preeclampsia'.<sup>44</sup> In current clinical practice, measuring resistance to flow in the uterine arteries is used to identify failure of trophoblast invasion into the spiral arteries<sup>31</sup> and to predict fetal IUGR and preeclampsia. Genetic and transplantation studies in mice have shown that uterine natural killer lymphocytes are essential for initiation of these structural changes in spiral arteries.<sup>15</sup> Murine spiral arteries that are undergoing these changes show decreased expression of cell markers of arteries and acquire those associated with veins.<sup>67</sup>

Pregnancy success also requires fetal and placental vasculogenesis followed by branching and nonbranching angiogenesis. The placentas of all mammals share common structural and functional features, but there are also striking differences between species in gross and microscopic structure of the placenta and its vasculature. The mouse fetoplacental circulation opens at approximately gestational day (gd) 9.<sup>13</sup> For both humans and mice, most pregnancy complications are associated with either decreased placental vascular development or obstruction to placental blood flow.<sup>46</sup> Both complications can be quantified by ultrasonography, as can changes in these parameters due to treatment, or in mice, experimental manipulations.

#### **Doppler ultrasonography of the maternal uterine artery.**

Through transabdominal and transvaginal scanning during various gestational stages, conventional Doppler ultrasonography of uterine and umbilical arteries is used widely to assess human fetoplacental circulation. Arterial waveforms are assessed by using color-power and pulsed Doppler imaging.<sup>30</sup> Transabdominal microultrasoundography has similarly been used to study flow patterns in mouse uterine arteries and the changes in flow patterns due to vascular remodelling during normal and compromised pregnancies (Figures 1, 2).<sup>42,70</sup> Pregnant mice typically are anesthetized by using isoflurane and restrained on a pivoting platform. Doppler waveforms of the mouse uterine arteries are collected by placing a 40-MHz probe (for example, RMV 704 [VisualSonics, Toronto, ON, Canada]) over the abdomen, where the fur has been removed by clipping or application of a depilatory. A 'coupling gel' usually is applied over the site being scanned. Images are collected over the lateral-caudal margin of the uterocervical junction close to the iliac artery on each side, ventral to the urinary bladder<sup>32</sup> (Figure 1 B).

Mice and humans demonstrate strong parallels in ultrasonographically-imaged placental structure, hemodynamics, and gene utilization<sup>12</sup> for normal pregnancies and those complicated by IUGR.<sup>2</sup> In nonpregnant and early (to gd9.5)-pregnant outbred Hsd:ICR (CD1) mice, a high-fecundity strain, the uterine artery blood velocity waveform was characterized by low end-diastolic velocity with a prominent diastolic notch. By gd15.5, after opening of the fetal circulation, uterine arteries had increased to peak

systolic and end-diastolic velocities, the calculated resistance index had decreased significantly, and the notch had disappeared.<sup>32</sup> In women, abnormal uterine artery waveforms are better predictors of preeclampsia than of IUGR. An increased pulsatility index alone or in combination with notching is most valuable for predicting IUGR in women at low risk of this fetal complication, whereas an increased resistance index is the best predictor of IUGR in mothers at high risk, such as those who are diabetic or hypertensive before becoming pregnant.<sup>10</sup>

Microultrasoundography has been used in the study of transgenic Sprague-Dawley rats harboring components of the human renin-angiotensin system (the [TGR(hRen)L10J] and TGR(hAogen)L1623 strains, respectively).<sup>17</sup> In this model of preeclampsia, female hAogen rats bred to hRen male rats developed hypertension and proteinuria in the second half of pregnancy. Microultrasoundography demonstrated a stable resistance index over pregnancy in the control, normotensive Sprague-Dawley rats<sup>17,58</sup> but an unexpected decrease in resistance index during pregnancy due to the mating of hypertensive rats, the fetuses of which became growth-restricted. From these data, the authors concluded that the poor fetal growth rate was not due to lack of placental perfusion. Clinical data, however, indicate that coordinated and sufficient uterine vascular remodeling is required for normal fetal growth.<sup>39</sup> These opposing conclusions may relate to differences in uterine hemodynamics and blood flow patterns due to litter-bearing in the rats.

We examined the gestational hemodynamics of normal (+/+) and alymphoid (*Rag2<sup>-/-</sup>/Il2rg<sup>-/-</sup>*) BALB/cAnNCrI female mice, in which spiral arterial remodeling does not occur due to their deficit in uterine natural killer cells.<sup>34</sup> For both genotypes, uterine artery flow velocity increased at midgestation (gd10) and remained high until late gestation (gd18.5) and pulsatility and resistance indices decreased significantly at gd9–10, as the placental circulation opened.<sup>66</sup> Combining microultrasoundography with monitoring of mean arterial pressure can improve our understanding of the changes in hemodynamic properties that occur during pregnancy. Others combined microultrasoundography with tail-cuff recording of mean arterial pressures revealed increases in heme oxygenase activity in maternal and placental tissues that contributed to the regulation of peripheral vascular resistance.<sup>69</sup> We have conducted experiments using microultrasoundography and continuous radiotelemetric recording of mean arterial pressure in parallel groups of BALB/cAnNCrI (H2d) and C57BL/6J (H2b) mice. Mean arterial pressure fell postimplantation (as occurs in women) to a nadir at gd9 and then rebounded gradually.<sup>14</sup> Microultrasoundography revealed a significant increase in uterine arterial flow concurrent with this rebound in arterial pressure.<sup>7</sup> The outcome of both of these mechanisms is increased perfusion of placental tissue and improved nutrient delivery to the growing fetus.

**Doppler ultrasonography of spiral arteries.** Unlike uterine arteries, spiral arteries are not constant in their anatomic positions and characteristics. Physiologic changes to the human spiral artery system are functionally complete about the 17th week of gestation. From measurements of term placentae, the average number of spiral arteries is thought to be close to 100.<sup>29</sup> In 1991, the emergence of color Doppler imaging improved measurements of human spiral arterial function during pregnancy. The waveforms in pregnant women indicated that in normal pregnancies, spiral arterial resistance to flow decreased progressively as gestation advanced.<sup>26</sup> Spiral arterial waveforms typically have a higher dia-

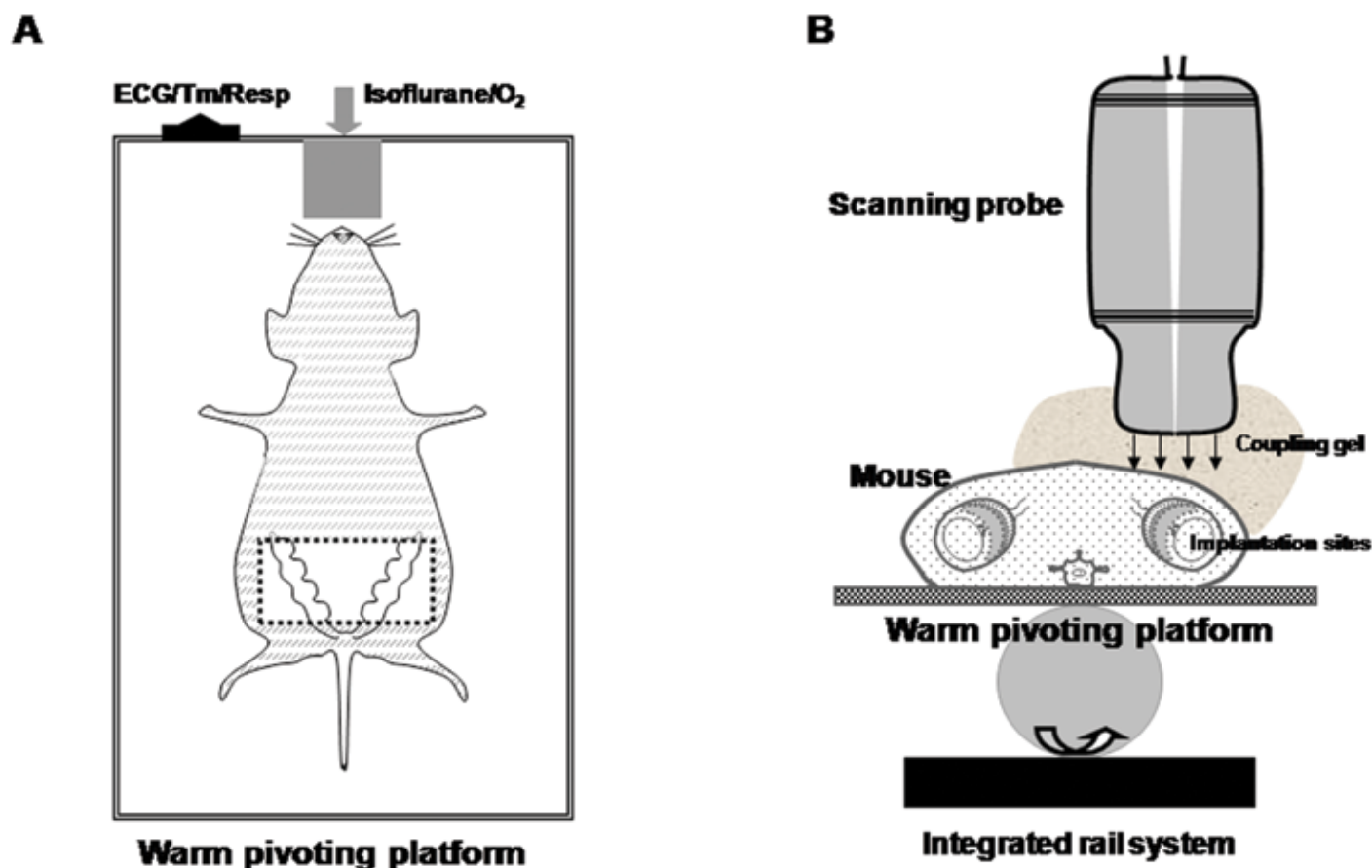


**Figure 1.** Positioning and ultrasound imaging of an anesthetized, dorsally recumbent pregnant mouse (A) as an aerial view and (B) in transverse cross-section. Studies can be performed on mice at different gestational stages. All hair was removed from the ventral abdomen after the mouse was anesthetized with approximately 2.0% (1.5% to 2.5%) isoflurane by means of an oxygen mask. The mouse then was placed on the platform and held in position with surgical tape. A thick layer of warm water-based coupling gel was applied over the skin of the area to be imaged. A 40-MHz transducer probe was applied to the skin to collect images. The transabdominal area (boxed region in A) is suitable for detection of the pregnant uterus. To acquire optimal images, the scanning probe needs to carefully be adjusted to the natural orientation of each implantation site. All waveforms are saved for later offline analysis. Maternal heart and respiration rates were monitored by using an automated system. Body temperature was maintained as 36 to 37 °C by the warmed platform, which is supported by an integrated rail system. Figures are not to scale.

stolic flow velocity (indicating a lower downstream resistance to flow) than does the uterine artery.

Normal mice have 5 to 10 spiral arteries located within the mesometrial triangle of each implantation site. Analysis of plastic vascular casts revealed that dilation of CD1 spiral arteries becomes apparent at gd10.5 and continues to gd14.5. On average, lumen diameter increased from 60  $\mu\text{m}$  to 150  $\mu\text{m}$ .<sup>3</sup> In CBA/J female mice mated by DBA/2J male mice, spiral artery lumen areas were estimated from histologic sections to increase from 0.019 to 0.041  $\text{mm}^2$  between gd10 and gd12; vessel area at these same time points was 0.042 and 0.065  $\text{mm}^2$ .<sup>68</sup> We histologically compared the average ratio of vessel diameter to lumen diameter for C57BL/6J<sup>+/+</sup> gestationally modified spiral arteries and the unmodified arteries of C57BL/6J *Rag2<sup>-/-</sup>/Il2rg<sup>-/-</sup>* mice. The ratio was 1.17 for the modified arteries and greater than 2 for those that were not modified.<sup>5</sup>

Mouse spiral arteries can be identified by Doppler microultrasoundography due to their characteristic waveforms (Figure 2 D). In late pregnancy, spiral arteries proximal to the myometrium have a much greater diastolic waveform than does the uterine artery.

At their distal ends (toward the placenta), spiral arteries show a venous-like wave pattern without pulsating peaks. An important unresolved issue is how to acquire accurate Doppler data of spiral arteries due to the variable waveforms, which reflect the contributions of variable amounts of residual vascular smooth muscle during the physiologic remodeling process. Increasing the numbers of measurements at different positions along the length of each vessel to acquire an average would be 1 approach. Alternatively, a constant ultrasound gate might be used to scan a fixed area in multiple animals.

**Placental and placental vascular measurements by 3D power Doppler ultrasonography.** Fetal size at birth is a critical contributor to life expectancy, affecting not only neonatal viability but also adult rates of mortality and morbidity.<sup>6</sup> Generally, there is a nonlinear but important predictive relationship between placenta weight and birth weight.<sup>48</sup> In normal human pregnancies, the placenta has a granular echotexture that first becomes visible by ultrasonography about the 8th week of pregnancy. Changes in echogenicity and the appearance of ultrasonography-detected calcifications are used to assess placental maturity. Measurements

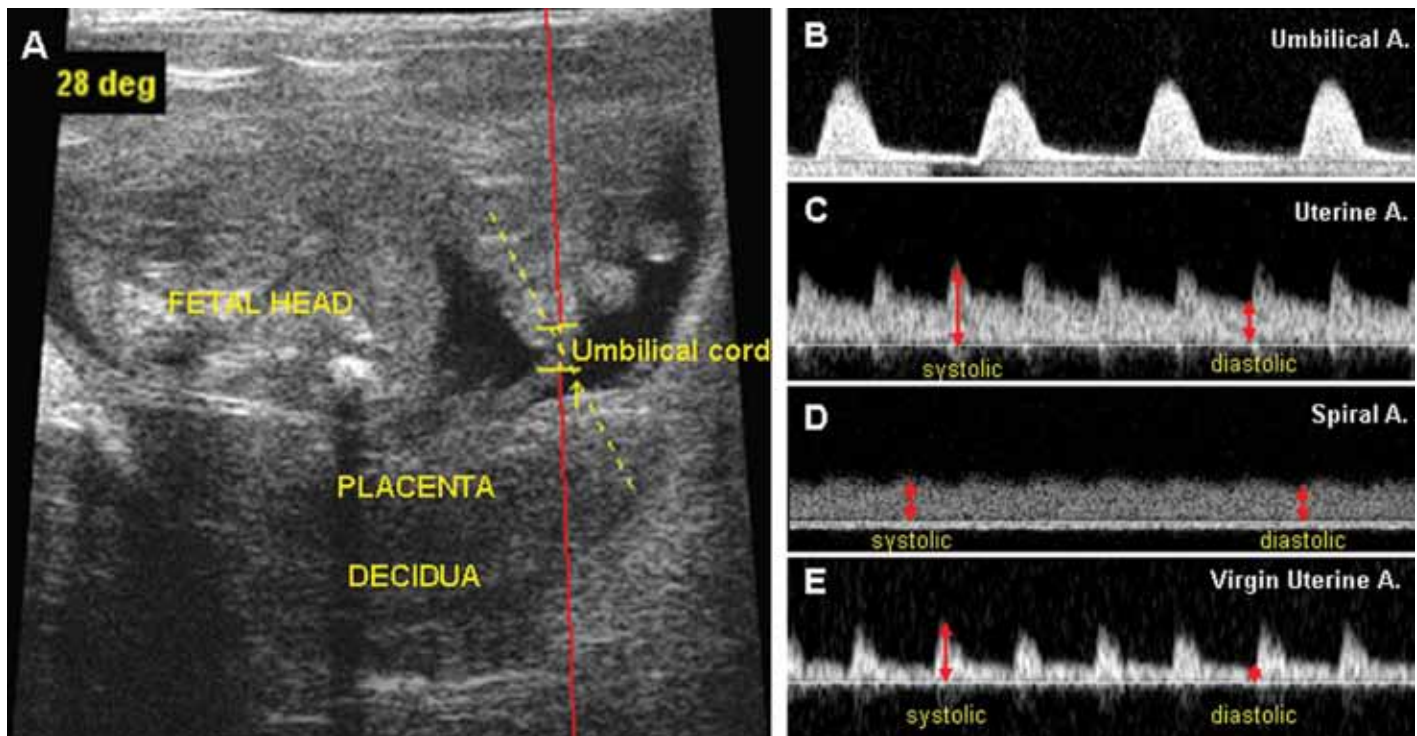


**Figure 2.** Examples of ultrasound microscope B-mode images from a gd16 BALB/cAnNCrl mouse. (A) Fetal, placental, and maternal decidual areas. The angle of the Doppler beam was less than 30°. Doppler velocity waveforms from the (B) umbilical artery, (C) uterine artery, and (D) transformed spiral artery are shown. (E) Compared with the flow pattern associated with pregnancy (panel C), the uterine artery of virgin BALB/c mice yielded a higher-resistance Doppler waveform. Comparing the time interval between systolic (or diastolic) peaks of the uterine artery and umbilical artery reveals that in mice, the fetal heart beat is much slower than the maternal heart beat. The reverse is seen in human pregnancy.<sup>49</sup> The difference between systolic and diastolic peaks (red lines in panels C and D) was greater in the source uterine artery than in its modified spiral artery tributary. These differences can be evaluated by multiple indices including pulsatility index, resistance index, ratio of systolic to diastolic flow, and so on. Pulse repetition frequency, 10 kHz; wall filter, 100 Hz; display window, 2000 ms; sound speed, 1540 m/s; Doppler gain, 5.00 DB. The red line in image A is a wire frame overlay for pulsed-wave Doppler ultrasonography.

of human placental size by ultrasonography were introduced about 20 y ago, after a report<sup>65</sup> stating that small placental volumes, estimated by 2-dimensional ultrasonography, were more common in cases of adverse pregnancy outcomes. However, rotational effects lead to high intra- and interobserver variability in volume measurements.<sup>35</sup> Recently, 3D ultrasonography has improved reproducibility in placental volume measurements.<sup>61</sup> The combination of power and color Doppler sonography detects blood movement in very small vessels and permits calculation of their effect on overall perfusion of a given placental volume. These indices are computed by using built-in algorithms or the VOCAL (Virtual Organ Computer-aided Analysis) program.<sup>23,38</sup> Volume measurements by 3D ultrasonography can be used to trisomies 13 and 18 that are associated with small placentae.<sup>61</sup> Others report that placental volume measurement is a more reliable predictor of neonatal size than is direct fetal measurement.<sup>53</sup>

Microultronography can be applied to murine pregnancy diagnosis and determination of litter size from very early stages of gestation.<sup>41</sup> We find reliable diagnosis from gd7.5 by using the Vevo 770 High-Resolution Imaging System (VisualSonics), but accurate estimation of litter size is complicated by the overlapping of implantation sites and mobility of the uterine horns. Microultronography has also been used to study mouse placental growth, with placental volume typically studied by placing the probe perpendicular to the long axis of each placenta. For our

equipment (RMV 704 Scanhead, catalog no. VS11170, VisualSonics), this placement did not resolve peripheral placental regions adequately, and transverse scanning provided an image with improved echogenicity (Figure 3). Because the placenta does not have an ideal geometric shape, manual machine control will give more accurate and sensitive volume assessments than automated analyses, even if the rotation angle was selected carefully. In CD1 mice, placental diameter and thickness increase nonlinearly between gd10.5–14.5 and then remain constant until term.<sup>33</sup> Published stereologic and measurements of C57BL/6J placentae estimate gd15.5 as the time when peak volume (0.104 cm<sup>3</sup>) and weight (942 mg) occur.<sup>11</sup> As in humans, microultronography reveals calcification of the maturing mouse placenta, which currently is considered to be a benign process that demarcates the maternal–fetal (that is decidua–trophoblast) boundary between gd7.5 to 9.5, prior to the completion of placental development. From gd15.5, sonography reveals calcification within the labyrinthine region of the mouse placenta, which is the highly vascular nutrient exchange area.<sup>4</sup>

In humans, reliable measurements of placental vascularity are obtained from anterior and posterior scanning until approximately 28 wk of gestation. Total reduced placental vascularity and impaired budding of the vascular tree in the placental villi can predict cases of preeclampsia and IUGR, which cannot be identified completely by either uterine or umbilical artery spec-

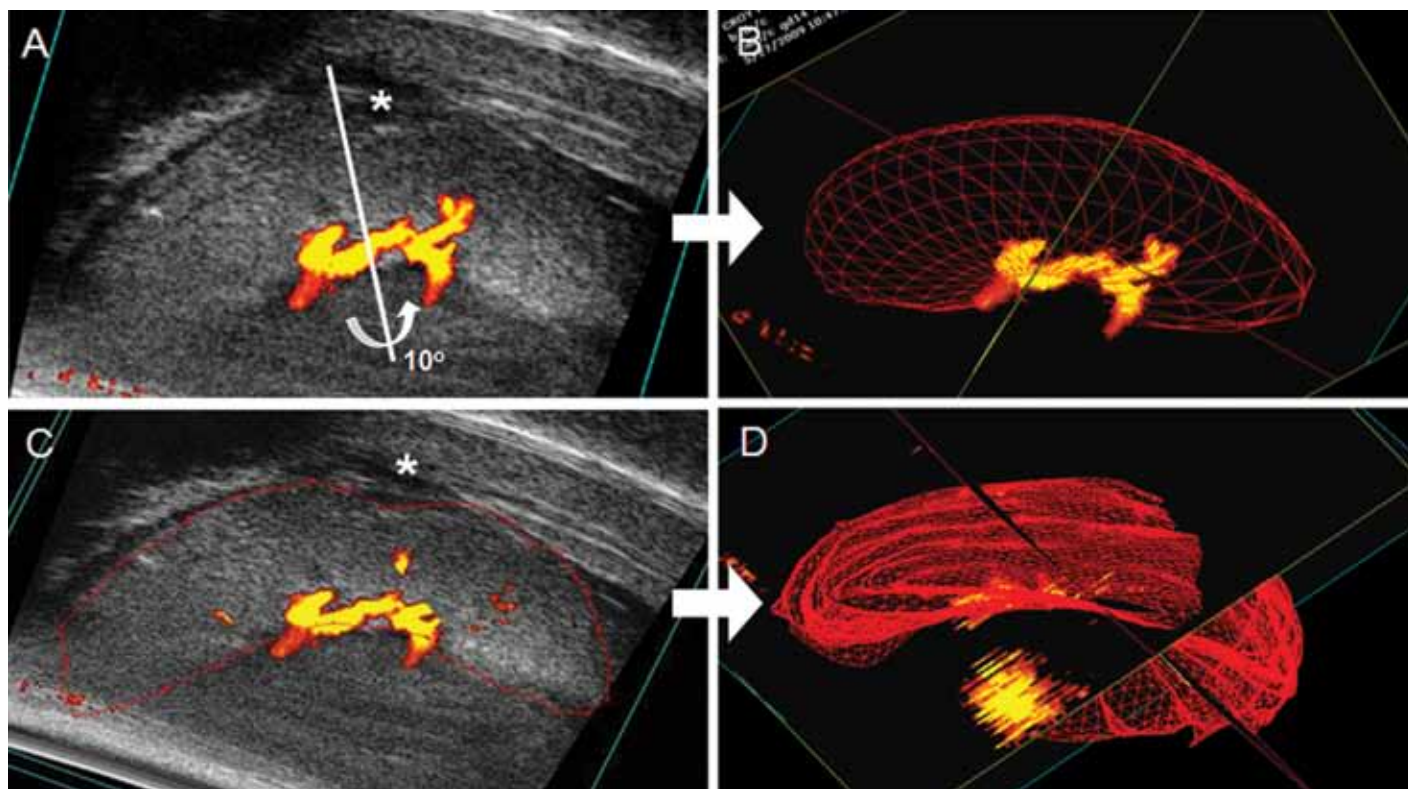


**Figure 3.** Volumetric measurement of the same gd14 BALB/cAnNCrl placenta by 2 techniques. After the parameters of the target scan area were set (step size, 0.1 mm; display at 20 to 30 dB), a 3D-mode image was acquired by using a 40-MHz probe. The 3D-mode volume tool was used in cube view (A and C) to measure the object volume of the placenta. For automated calculation of rotational segmentation (A, B), a rotational axis (white bar) was set manually, and a 3D image representative of the volume around the axis was created (B). This image usually excluded the edges of the placental disc and did not account for irregularities in shape. For the manual, parallel serial collection of volume estimate, a manual outline of the placenta was drawn (red), and a series of contours and calculations of volume within each contour was built. The resulting, integrated parallel segmentation 3D image is shown in (D). Typically, rotational segmentation should be used only when the volume has ideal geometric shape. Panels A and C show irregular contours (\*) on the placenta. The yellow central component of each image is the Doppler flow within the umbilical cord; the red edges are regions of slower flow.

tral waveforms.<sup>47</sup> In the 3rd trimester, visualization of the villous circulation becomes more difficult due to shadowing of the posterior placenta by the fetus.<sup>8,45</sup> Placental vascular sonobiopsy may provide new information on the assessment of placental vascularization in normal pregnancies and those associated with fetal growth restriction. Weak linear relationships exist between gestational age and the vascularization index, flow index, and vascularization flow index.<sup>37</sup> To evaluate the vasculature of the mouse placenta, arterial and venous waveforms are compared. The arterial side of the vasculature shows coincident peaks with fetal heart beats whereas veins lack these peaks. Umbilical diameters (artery or vein) in CD-1 mice did not differ between gd13.5 to 15.5, whereas placental arterial surface area had significantly increased by gd18.5; venous surface areas were enlarged in parallel but always to a lesser extent.<sup>45</sup> Our preliminary data from C57BL/6J and BALB/cAnNCrl pregnancies also indicate that placental thickness, diameter, volume, and vascular density increase throughout gestation.<sup>66</sup>

**Quality assessment and improvement.** Doppler studies of pregnancy are well established for clinical and research use in humans and many livestock species. Their introduction for small rodents has been an important advance for studies of developmental and pregnancy biology. Because Doppler ultrasonography measures

the amplitude of scattering of ultrasound waves, it is influenced by a number of factors including the machine settings of gain, filter, and beam path and frequency and has limitations.<sup>62</sup> Currently, only microvessels in the range of 30 to 100  $\mu\text{m}$  are detected clinically and those in the range of 15 to 20  $\mu\text{m}$  by microultrasonography. Detection of slowly flowing blood remains difficult even in highly resolved vessels because of the properties of filters that are required to discriminate such flow from vessel wall, heart, and breathing motions.<sup>22,27</sup> Therefore improvement in machine sensitivity is important to quantification of the state of blood flow.

Technologic developments are continuing to improve rodent microultrasonography. Contrast-enhanced ultrasonography can provide more information than do conventional methods.<sup>51,64</sup> The use of microbubbles enhances the backscatter or reflection of probe-generated ultrasound waves, producing a sonogram with improved image quality.<sup>20,63</sup> New microscan transducers<sup>60</sup> increase frame rate collection and have multiple focus planes, thus providing superior contrast and more detailed resolution over a wider field of view. Software upgrades also continue. With the availability of microultrasonography and other advanced imaging technologies, a new era has emerged for direct and comparative studies of the rodent maternal fetal interface.<sup>1,25,28,40,45</sup> The insights that mouse studies have provided are exciting not only

because they provide the foundation for analyses of mutant and manipulated mouse strains but also because of the real possibility that they will provide clues into unresolved complications of human pregnancy.<sup>9</sup>

## Acknowledgments

We thank Jalna Meens and Jeff Mewburn (Queen's Cancer Research Institute, Kingston, Ontario) for technical assistance regarding our ultrasonography research. We are also grateful to the Animal Care staff of Queen's University for their dedicated care of our immunodeficient mice and for their assistance in the design and implementation of the standard operating procedures that provide biosecurity to these animals during use of our institutional core microultrasonography facility. These studies were supported by the Natural Sciences and Engineering Research Council, Canada; Canadian Institutes of Health Research; and the Canada Research Chairs Program.

## References

1. **Abramowicz JS, Sheiner E.** 2007. In utero imaging of the placenta: importance for diseases of pregnancy. *Placenta* **28**:S14–S22.
2. **Adamson SL.** 2007. Placental vascular disease in mouse models of intrauterine growth restriction. *Biol Reprod* **77**:69–b–69.
3. **Adamson SL, Lu Y, Whiteley KJ, Holmyard D, Hemberger M, Pfarrer C, Cross JC.** 2002. Interactions between trophoblast cells and the maternal and fetal circulation in the mouse placenta. *Dev Biol* **250**:358–373.
4. **Akirav C, Lu Y, Mu J, Qu DW, Zhou YQ, Slevin J, Holmyard D, Foster FS, Adamson SL.** 2005. Ultrasonic detection and developmental changes in calcification of the placenta during normal pregnancy in mice. *Placenta* **26**:129–137.
5. **Ashkar AA, Di Santo JP, Croy BA.** 2000. Interferon gamma contributes to initiation of uterine vascular modification, decidual integrity, and uterine natural killer cell maturation during normal murine pregnancy. *J Exp Med* **192**:259–270.
6. **Barker DJP.** 2002. Fetal programming of coronary heart disease. *Trends Endocrinol Metab* **13**:364–368.
7. **Burke SD, Barrette V F, Bianco J, Thorne JG, Yamada AT, Pang SC, Adams MA, Croy BA.** 2009. Spiral arterial remodeling is not essential for normal blood pressure regulation in pregnant mice. Submitted.
8. **Campbell S.** 2007. Placental vasculature as visualized by 3D power Doppler angiography and 3D color Doppler imaging. *Ultrasonography Obstet Gynecol* **30**:917–920.
9. **Carson PL, Fenster A.** 2009. Evolution of ultrasound physics and the role of medical physicists and the AAPM and its journal in that evolution. *Med Phys* **36**:411–428.
10. **Nossen JS, Morris RK, ter Riet G, Mol B, van der Post JA, Coomarasamy A, Zwinderman AH, Robson SC, Bindels PJ, Kleijnen J, Khan KS.** 2008. Use of uterine artery doppler ultrasonography to predict preeclampsia and intrauterine growth restriction: a systematic review and bivariable meta-analysis. *CMAJ* **178**:701–711.
11. **Coan PM, Ferguson-Smith AC, Burton GJ.** 2004. Developmental dynamics of the definitive mouse placenta assessed by stereology. *Biol Reprod* **70**:1806–1813.
12. **Cox B, Kotlyar M, Evangelou AI, Ignatchenko V, Ignatchenko A, Whiteley K, Jurisica I, Adamson SL, Rossant J, Kislinger T.** 2009. Comparative systems biology of human and mouse as a tool to guide the modeling of human placental pathology. *Mol Syst Biol* **5**:279.
13. **Cross JC, Hemberger M, Lu Y, Nozaki T, Whiteley K, Masutani M, Adamson SL.** 2002. Trophoblast functions, angiogenesis, and remodeling of the maternal vasculature in the placenta. *Mol Cell Endocrinol* **187**:207–212.
14. **Croy BA, Barrette VF, Laverty K, Thorne JG, Adams MA.** 2008. Blood pressure regulation during mouse pregnancy is independent of spiral arterial modification. *International Society for the Study of Hypertension in Pregnancy*. Washington (DC). 21–24 September 2008.
15. **Croy BA, van den Heuvel MJ, Borzychowski AM, Tayade C.** 2006. Uterine natural killer cells: a specialized differentiation regulated by ovarian hormones. *Immunol Rev* **214**:161–185.
16. **David AL, Torondel B, Zachary I, Wigley V, Nader KA, Mehta V, Buckley SMK, Cook T, Boyd M, Rodeck CH, Martin J, Peebles DM.** 2008. Local delivery of VEGF adenovirus to the uterine artery increases vasorelaxation and uterine blood flow in the pregnant sheep. *Gene Ther* **15**:1344–1350.
17. **Dechend R, Gratzke P, Wallukat G, Shagdarsuren E, Plehm R, Brasen J-H, Fiebeler A, Schneider W, Caluwaerts S, Vercruyse L, Pijnenborg R, Luft FC, Muller DN.** 2005. Agonistic autoantibodies to the AT1 receptor in a transgenic rat model of preeclampsia. *Hypertension* **45**:742–746.
18. **Donald I, Macvicar J, Brown TG.** 1958. Investigation of abdominal masses by pulsed ultrasound. *Lancet* **1**:1188–1195.
19. **Dumont O, Pinaud F, Guihot A-L, Baufreton C, Loufrani L, Henrion D.** 2007. Alteration in flow (shear stress)-induced remodelling in rat resistance arteries with aging: improvement by a treatment with hydralazine. *Cardiovasc Res* **77**:600–608.
20. **Ferrara K, Pollard R, Borden M.** 2007. Ultrasound microbubble contrast agents: fundamentals and application to gene and drug delivery. *Annu Rev Biomed Eng* **9**:415–447.
21. **Foster FS, Zhang MY, Zhou YQ, Liu G, Mehi J, Cherin E, Harasiwicz KA, Starkoski BG, Zan L, Knapik DA, Adamson SL.** 2002. A new ultrasound instrument for in vivo microimaging of mice. *Ultrasound Med Biol* **28**:1165–1172.
22. **Goertz DE, Yu JL, Kerbel RS, Burns PN, Foster FS.** 2003. High-frequency 3D color-flow imaging of the microcirculation. *Ultrasound Med Biol* **29**:39–51.
23. **Guiot C, Gaglioti P, Oberto M, Piccoli E, Rosato R, Todros T.** 2008. Is three-dimensional power Doppler ultrasound useful in the assessment of placental perfusion in normal and growth-restricted pregnancies? *Ultrasound Obstet Gynecol* **31**:171–176.
24. **Hangiandreou NJ.** 2003. AAPM/RSNA physics tutorial for residents. *Topics in US: B-mode US: basic concepts and new technology*. *Radiographics* **23**:1019–1033.
25. **Israel GM, Malguria N, McCarthy S, Copel J, Weinreb J.** 2008. MRI versus ultrasound for suspected appendicitis during pregnancy. *J Magn Reson Imaging* **28**:428–433.
26. **Jurkovic D, Jauniaux E, Kurjak A, Hustin J, Campbell S, Nicolaides KH.** 1991. Transvaginal color Doppler assessment of the uteroplacental circulation in early pregnancy. *Obstet Gynecol* **77**:365–369.
27. **Loveless ME, Li X, Huamani J, Lyshchik A, Dawant B, Hallahan D, Gore JC, Yankeelov TE.** 2008. A method for assessing the microvasculature in a murine tumor model using contrast-enhanced ultrasonography. *J Ultrasound Med* **27**:1699–1709.
28. **Luker GD, Luker KE.** 2008. Optical imaging: current applications and future directions. *J Nucl Med* **49**:1–4.
29. **Lyall F.** 2005. Priming and remodelling of human placental bed spiral arteries during pregnancy—a review. *Placenta* **26**:S31–S36.
30. **McLeod L.** 2008. How useful is uterine artery doppler ultrasonography in predicting preeclampsia and intrauterine growth restriction? *Can Med Assoc J* **178**:727–729.
31. **Melchiorre K, Leslie K, Prefumo F, Bhide A, Thilaganathan B.** 2009. First-trimester uterine artery Doppler indices in the prediction of small-for-gestational age pregnancy and intrauterine growth restriction. *Ultrasound Obstet Gynecol* **33**:524–529.
32. **Mu J, Adamson SL.** 2006. Developmental changes in hemodynamics of uterine artery, utero-, and umbilicoplacental, and vitelline circulations in mouse throughout gestation. *Am J Physiol Heart Circ Physiol* **291**:H1421–H1428.
33. **Mu J, Slevin J, Qu D, McCormick S, Adamson SL.** 2008. In vivo quantification of embryonic and placental growth during gestation in mice using microultrasound. *Reprod Biol Endocrinol* **6**:34.
34. **Murphy SP, Tayade C, Ashkar AA, Hatta K, Zhang J, Croy BA.** 2009. Interferon gamma in successful pregnancies. *Biol Reprod* **80**:848–859.

35. Nardoza LMM, Nowak PM, Araujo Junior E, Guimares Filho HA, Rolo LC, Torloni MR, Moron AF. 2009. Evaluation of placental volume at 7–10 + 6 weeks of pregnancy by 3D sonography. *Placenta* 30:585–589.
36. Naruse K, Lash GE, Innes BA, Otun HA, Searle RF, Robson SC, Bulmer JN. 2008. Localization of matrix metalloproteinase (MMP) 2, MMP9, and tissue inhibitors for MMPs (TIMPs) in uterine natural killer cells in early human pregnancy. *Hum Reprod* 24: 553–561.
37. Noguchi J, Hata K, Tanaka H, Hata T. 2009. Placental vascular sonobiopsy using 3-dimensional power Doppler ultrasound in normal and growth restricted fetuses. *Placenta* 30:391–397.
38. Nowak PM, Nardoza LMM, Araujo Junior E, Rolo LC, Moron AF. 2008. Comparison of placental volume in early pregnancy using multiplanar and VOCAL methods. *Placenta* 29:241–245.
39. Osol G, Mandala M. 2009. Maternal uterine vascular remodeling during pregnancy. *Physiology (Bethesda)* 24:58–71.
40. Pallares P, Fernandez-Valle ME, Gonzalez-Bulnes A. 2009. In vivo virtual histology of mouse embryogenesis by ultrasound biomicroscopy and magnetic resonance imaging. *Reprod Fertil Dev* 21:283–292.
41. Pallares P, Gonzalez-Bulnes A. 2009. Use of ultrasound imaging for early diagnosis of pregnancy and determination of litter size in the mouse. *Lab Anim* 43:91–95.
42. Pavlin CJ, Simpson ER, Foster FS. 2008. Ultrasound biomicroscopy. *Ultrasound Clin* 3:185–194.
43. Pijnenborg R, Vercruyse L, Hanssens M. 2006. The uterine spiral arteries in human pregnancy: facts and controversies. *Placenta* 27:939–958.
44. Redman CW, Sargent IL. 2005. Latest advances in understanding preeclampsia. *Science* 308:1592–1594.
45. Rennie MY, Whiteley KJ, Kulandavelu S, Adamson SL, Sled JG. 2007. 3D visualisation and quantification by microcomputed tomography of late gestational changes in the arterial and venous fetoplacental vasculature of the mouse. *Placenta* 28:833–840.
46. Reynolds LP, Borowicz PP, Vonnahme KA, Johnson ML, Grazul-Bilska AT, Wallace JM, Caton JS, Redmer DA. 2005. Animal models of placental angiogenesis. *Placenta* 26:689–708.
47. Reynolds LP, Caton JS, Redmer DA, Grazul-Bilska AT, Vonnahme KA, Borowicz PP, Luther JS, Wallace JM, Wu G, Spencer TE. 2006. Evidence for altered placental blood flow and vascularity in compromised pregnancies. *J Physiol* 572:51–58.
48. Sanin LH, Lopez SR, Olivares ET, Terrazas MC, Silva MAR, Carrillo ML. 2001. Relation between birth weight and placenta weight. *Biol Neonate* 80:113–117.
49. Serra V, Bellver J, Moulden M, Redman CWG. 2009. Computerized analysis of normal fetal heart rate pattern throughout gestation. *Ultrasound Obstet Gynecol* 34:74–79.
50. Smith SD, Dunk CE, Aplin JD, Harris LK, Jones RL. 2009. Evidence for immune cell involvement in decidual spiral arteriole remodeling in early human pregnancy. *Am J Pathol* 174:1959–1971.
51. Song IH, Althoff CE, Hermann KG, Scheel AK, Knetsch T, Burmester GR, Backhaus M. 2009. Contrast-enhanced ultrasound in monitoring the efficacy of a bradykinin receptor 2 antagonist in painful knee osteoarthritis compared with MRI. *Ann Rheum Dis* 68:75–83.
52. Tayade C, Hilchie D, He H, Fang Y, Moons L, Carmeliet P, Foster RA, Croy BA. 2007. Genetic deletion of placenta growth factor in mice alters uterine NK cells. *J Immunol* 178:4267–4275.
53. Thame M, Osmond C, Wilks R, Bennett FI, Forrester TE. 2001. Second-trimester placental volume and infant size at birth. *Obstet Gynecol* 98:279–283.
54. Torry DS, Leavenworth J, Chang M, Maheshwari V, Groesch K, Ball ER, Torry RJ. 2007. Angiogenesis in implantation. *J Assist Reprod Genet* 24:303–315.
55. van der Heijden OWH, Essers YPG, Fazzi G, Peeters LLH, De Mey JGR, van Eys GJJM. 2005. Uterine artery remodeling and reproductive performance are impaired in endothelial nitric oxide synthase-deficient mice. *Biol Reprod* 72:1161–1168.
56. van der Heijden OWH, Essers YPG, Simkens LHJ, Teunissen QGA, Peeters LLH, De Mey JGR, van Eys GJJM. 2004. Aging blunts remodeling of the uterine artery during murine pregnancy. *J Soc Gynecol Investig* 11:304–310.
57. van der Heijden OWH, Essers YPG, Spaanderma MEA, De Mey JGR, van Eys GJJM, Peeters LLH. 2005. Uterine artery remodeling in pseudopregnancy is comparable to that in early pregnancy. *Biol Reprod* 73:1289–1293.
58. Verlohren S, Niehoff M, Hering L, Geusens N, Herse F, Tintu AN, Plagemann A, LeNoble F, Pijnenborg R, Muller DN, Luft FC, Dudenhausen JW, Gollasch M, Dechend R. 2008. Uterine vascular function in a transgenic preeclampsia rat model. *Hypertension* 51:547–553.
59. Villar J, Carroli G, Wojdyla D, Abalos E, Giordano D, Ba'aqel H, Farnot U, Bergsj P, Bakketeig L, Lumbiganon P, Campodonico L, Al-Mazrou Y, Lindheimer M, Kramer M. 2006. Preeclampsia, gestational hypertension, and intrauterine growth restriction: related or independent conditions? *Am J Obstet Gynecol* 194:921–931.
60. VisualSonics. [Internet]. Vevo 2100: a whole new dimension in preclinical imaging intelligence. [Cited Aug 13 2009]. Available at <http://www.visualsonics.com/vevo2100/newdimension.htm>.
61. Wegrzyn P, Faro C, Falcon O, Peralta CFA, Nicolaides KH. 2005. Placental volume measured by three-dimensional ultrasound at 11 to 13 + 6 weeks of gestation: relation to chromosomal defects. *Ultrasound Obstet Gynecol* 26:28–32.
62. Welsh AW. 2008. A caution regarding standardization of power Doppler to measure perfusion in placental tissue. *Ultrasound Obstet Gynecol* 31:111–112.
63. Willmann JK, Cheng Z, Davis C, Lutz AM, Schipper ML, Nielsen CH, Gambhir SS. 2008. Targeted microbubbles for imaging tumor angiogenesis: assessment of whole-body biodistribution with dynamic microPET in mice. *Radiology* 249:212–219.
64. Wilson SR, Burns PN. 2006. Microbubble contrast for radiological imaging 2. Applications. *Ultrasound Q* 22:15–18.
65. Wolf H, Oosting H, Treffers PE. 1989. Second-trimester placental volume measurement by ultrasound: prediction of fetal outcome. *Am J Obstet Gynecol* 160:121–126.
66. Zhang J, Croy BA. 2009. Ultrasound characterization of maternal and fetal blood flow in mice with normal or absent spiral arterial modification. 33rd Annual Perinatal Investigators Meeting, Kingston, Canada, 12-13 November 2009.
67. Zhang J, Dong H, Wang B, Zhu S, Croy BA. 2008. Dynamic changes occur in patterns of endometrial EFNB2/EPHB4 expression during the period of spiral arterial modification in mice. *Biol Reprod* 79:450–458.
68. Zhang J, Wei H, Wu D, Tian Z. 2007. Toll-like receptor 3 agonist induces impairment of uterine vascular remodeling and fetal losses in CBA x DBA/2 mice. *J Reprod Immunol* 74:61–67.
69. Zhao H, Wong RJ, Doyle TC, Nayak N, Vreman HJ, Contag CH, Stevenson DK. 2008. Regulation of maternal and fetal hemodynamics by heme oxygenase in mice. *Biol Reprod* 78:744–751.
70. Zhou YQ, Foster FS, Qu DW, Zhang M, Harasiewicz KA, Adamson SL. 2002. Applications for multifrequency ultrasound biomicroscopy in mice from implantation to adulthood. *Physiol Genomics* 10:113–126.
71. Zygmunt M, Herr F, Munstedt K, Lang U, Liang OD. 2003. Angiogenesis and vasculogenesis in pregnancy. *Eur J Obstet Gynecol Reprod Biol* 110:S10–S18.